EXPERIMENTAL AND FINITE ELEMENT FATIGUE ASSESSMENT OF THE SPRING CLIP OF THE SKL-1 RAILWAY FASTENING SYSTEM

Diego Ferreño[1*], José Antonio Casado[1], Isidro Alfonso Carrascal[1], Soraya Diego[1], Estela Ruiz[1], María Saiz[1], José Adolfo Sainz-Aja[1], Ana Isabel Cimentada[1].

[1] LADICIM (Laboratory of Science and Engineering of Materials), University of Cantabria. E.T.S. de Ingenieros de Caminos, Canales y Puertos, Av. Los Castros 44, 39005 Santander, Spain.

*Corresponding author: Diego Ferreño. Phone: +34 682 840 956; e-mail: ferrenod@unican.es

Abstract

The fastening system that links the rail and the sleeper in railway lines is an element of high responsibility, since its failure may lead to the derailment of the train. This paper combines an experimental approach and a Finite Element model to assess the structural integrity of the spring clip of the SKL-1 fastening system, used assiduously in high-speed lines. Our results prove that fatigue is not the failure mechanism that explains the fractures of clips as pointed out by other authors, provided the following requirements: the material has received the appropriate thermomechanical treatments during; the assembly of the clip has been carried out with precision; and the system has not suffered anomalous in-service overloads.

Keywords: Railway fastening system; Finite Element; fatigue test; failure analysis; steel spring clip.

1.- INTRODUCTION

Rail transport has experienced a remarkable boost in recent decades. In particular, high-speed rail has accounted for a substantial fraction of public transport investments in many Western countries and in China. At present, high-speed trains can circulate at 350 km/h. However, public managers aspire to increase the in-service speed even more, in order to improve the quality of

the transport. This would represent a technological challenge in many aspects, in particular with regard to the forces supported by the fastening system that connects the rails and the sleepers and transmits the static and dynamic forces exerted by the passing stocks to the railway infrastructure. The fastening system maintains the gauge of the track and the inclination of the rails within the admissible tolerances avoiding the overturning of the rail. The SKL-1 fastening system, developed by Vossloh™, see Fig. 1, is used assiduously on high-speed as well as on some conventional tracks.

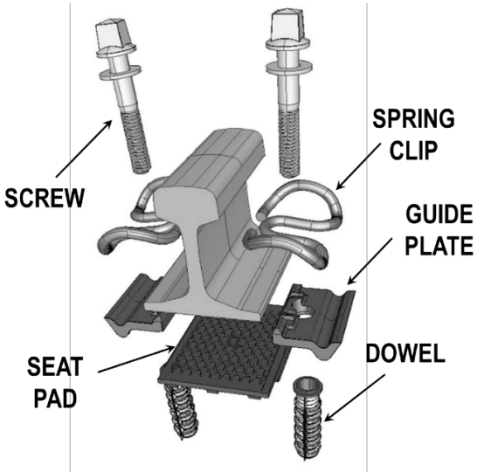

Figure 1. Schematic description of the SKL-1 fastening system and its components.

The literature reports examples of failure of fastening spring clips detected during the inspections carried out on the tracks. These failures could compromise the very functionality of the railway and the safety of vehicles and passengers. For this reason, it is necessary to identify the underlying causes. Lakusic et al. [1], reported several fractures of SKL-1 fastening clips. These authors developed a Finite Element (FE) model of the clip to determine the distribution and concentration of stresses subjected to in-service conditions. Their work presented several limitations such as the number of elements of the FE model, the simplified description of the properties of the material or the fact that they did not provide any experimental validation of the model. In addition, their research did not investigate the mechanisms that led to the breaking of the clips. Fatigue represents the most common mechanism of failure in structural components.

There is a large number of contributions dealing with fatigue assessment in railway components such as [2] [3] [4] [5]. For instance, in a recent contribution, Hong et al. [6] identified fatigue as the failure mechanism leading to the frequent fractures appearing in e-type spring clips in Beijing subway lines, jeopardizing the operational safety. They used a FE model to assess the fatigue life of an e-type fastening clip. The mechanical behavior of the 60Si2Mn spring steel was described by means of an elastic-plastic bilinear tensile curve (including hardening) [7] [8]. Based on this FE model, Hong et al. developed a complete parametric study of the clips in order to optimize their fatigue performance.

In this work, we have developed a FE numerical model (using the ANSYS Workbench 18.0 software) reproducing the operating conditions of the W-type clips of the SKL-1 fastening system. The study has been carried out in three different phases. In a first stage, the mechanical behavior of the 38Si7 steel of the clip was characterized. To this end, standardized specimens were heat treated and shot-peened (like the actual spring clips), and subjected to tensile tests (to obtain the mechanical properties) and fatigue tests (to determine the P-S-N curves, i.e., conventional fatigue S-N curves but including the probability of failure, P).). In a second phase, the behavior of the clip was characterized through quasi-static and fatigue tests, respectively. The experimental results were used to calibrate and validate the FE model (both under static and fatigue loading). Finally, once the numerical model was validated, it was used to simulate the response of the component under in-service conditions, in order to assess its structural integrity when subjected to fatigue loading.

2. MATERIAL AND METHODS

2.1. MATERIAL

SKL-1 clips are fabricated in 38Si7 steel. Its specified chemical composition is detailed in Table 1 [9].

Table 1. Chemical composition of the clip (% wt.)

C	Si	Mn	S	P
0.37 - 0.44	1.5 - 1.9	0.6 – 0.8	<0.04	<0.04

The manufacture of the W-type clips consists of the mechanical forming of the wire rod followed by a quenching and annealing heat treatment (quenching in water from 910ºC and annealing at 455ºC for one hour) followed by a shot-peening (to reduce the susceptibility of the material to fatigue) [10]. To faithfully reproduce the response of the steel, two standard tensile specimens and 27 standard fatigue specimens were machined from wire rod to determine, respectively, the mechanical properties and the fatigue behavior (P-S-N curves) of the steel. After machining the specimens, one of the tensile specimens was subjected to the aforementioned heat and shot-peening treatments at the same facilities employed to manufacture the clips. The non-treated tensile specimen was used to observe the influence of the treatments on the material mechanical response.

For the validation of the FE models, 13 actual SKL-1 clips were manufactured for this research and tested under different conditions. One of them was subjected to a quasi-static compression test obtaining the load-displacement curve. The remaining 12 clips were fatigue loaded, recording the number of cycles to failure. In both cases, the predictions derived from the FE models were compared to the experimental response. Finally, a series of tests have been carried out on a complete fastening system. The loads were applied on the rail, simulating the passage of a train, recording various relevant displacements experienced by the whole assembly that were subsequently employed as boundary conditions for a FE model of the system. In light of the experimental and numerical results obtained, an assessment of the possible fatigue failure of a fastening spring clip under in-service conditions has been carried out.

2.2.- EXPERIMENTAL SCOPE ON STANDARD SPECIMENS

2.2.1.- MICROHARDNESS TESTS

To verify the representativeness of the experimental results derived from tensile and fatigue tests performed on standard specimens, it is necessary to guarantee that their final mechanical properties, after thermal and shot-peening treatments, agree with those of the actual SKL-1 clips. For this reason, small coupons were extracted from the ends of the tensile and fatigue samples and Vickers microhardness profiles were obtained. This same procedure has been carried out on coupons extracted from the ends of the W-type clips. Subsequently, the results have been compared to verify the representativeness of the material constituting the standardized specimens. The microhardness tests have been carried out with a Neurtek microdurometer model Qness Q10-30-60, applying a load of 25 gf for 20 s following the procedure established in the standard ASTM E 92-17 [11]

2.2.2.- TENSILE TESTS

The tensile tests have been carried out in an Instron 8501 Universal servo hydraulic machine with a loading capacity of 100 kN and following the procedure of the standard ASTM E 8M-16 [12].

2.2.3.- FATIGUE TESTS

The fatigue tests on specimens have allowed the P-S-N curves of the material to be obtained; that is, the curves that relate the number of cycles to fracture (N) as a function of the stress amplitude ($S \equiv \sigma_a$) applied for a given failure probability (P). These tests have been carried out by means of a Servohydraulic Universal Instron 8501 test machine with a loading capacity of 100 kN and following the requirements of the ASTM E466-96 standard [13]. To describe the uncertainty inherent to fatigue, the confidence bands (associated with various probabilities of failure) of the experimental data were determined using the statistical module of the MATLAB™ software. For the fatigue characterization, two types of loading conditions have been imposed: 13 of the specimens were tested maintaining a stress ratio $R = \sigma_{min} / \sigma_{max} = -1$ (which is the reference

condition to obtain the SN curves) while R = 0.1 was imposed for the remaining 14 samples. As will become evident later, having experimental results obtained from two values of R (R=-1 and R=0.1, respectively) will make it possible to identify the model to correct the effect induced by the mean stress during fatigue.

2.3.- EXPERIMENTAL SCOPE ON SKL-1 CLIPS

2.3.1.- QUASI-STATIC TEST

As sketched in Fig. 2(a), this test consists in fixing the central region of the clip (which is in contact with the bolt) and compressing its ends (in contact with the rail), applying the force F, to obtain the load-displacement curve of the component. The test was carried out under load control by means of an Instron 8500 Universal servohydraulic machine, with a loading capacity of 250 kN and following the procedure DBS 918 127 [14]. First, the clip is compressed to a maximum force of 25 kN and then completely unloaded. Fig. 2(b) shows a photograph of the test carried out where the LVDT used to record the displacements can be seen. The experimental results obtained from this test were employed as a first criterion to validate de FE model (see section 3.3.1).

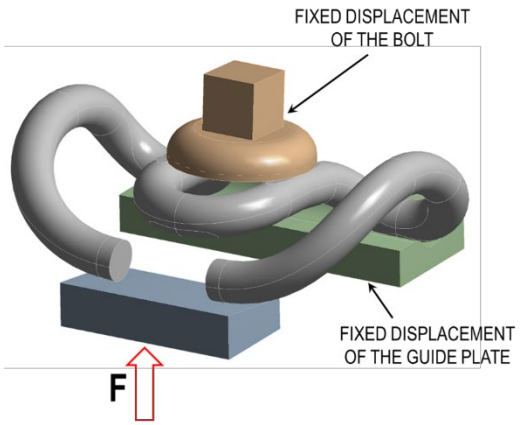

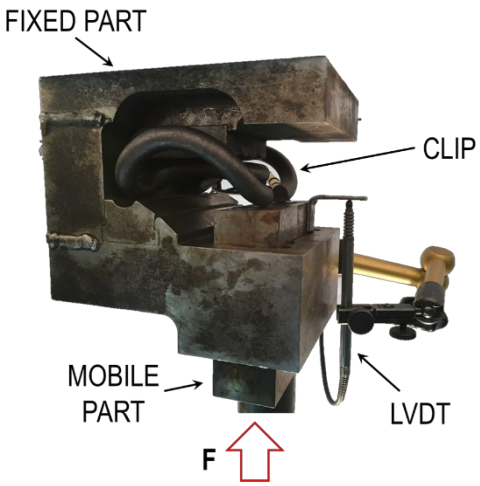

(a)

(b)

Figure 2. (a) Schematic description of the boundary conditions imposed in the quasi-static test of the clip. (b) Picture showing the performance of the test on an SKL-1 spring.

2.3.2.- FATIGUE TESTS

The boundary conditions of the fatigue tests consists in fixing the central region of the clip and compressing the ends, see Fig. 3. Fatigue tests were carried out by means of a servohidraulic Universal Instron 8501 testing machine, with a loading capacity of 100 kN, following the technical specification ET 03.360.566.8-Clips-ADIF [9]. The average force was F_m=2.5 kN and the force amplitude $F_a = (F_{max} – F_{min})/2$ ranged between 2 and 1.2 kN, see Table 2. As explained above, the validation of the FE model requires reproducing these results from the mechanical and fatigue properties of the material (see section 3.3.2).

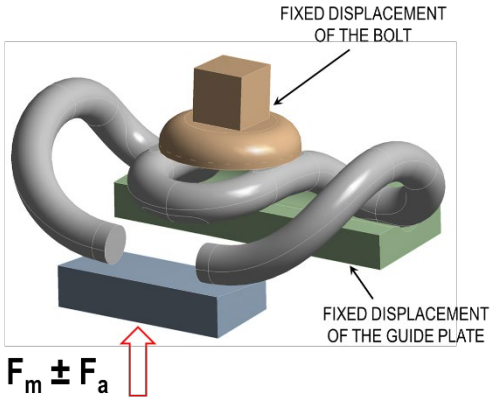

Figure 3. Schematic description of the boundary conditions imposed in the fatigue tests of the clips.

Table 2: Parameters of the fatigue tests carried out of SKL-1 spring clips.

F_a (kN)	F_{max} (kN)	F_{min} (kN)	# tests
2	4.5	0.5	2

1.8	4.3	0.7	2
1.7	4.2	0.8	2
1.6	4.1	0.9	2
1.3	3.8	1.2	2
1.2	3.7	1.3	2

2.3.3.- REPRODUCTION OF IN-SERVICE CONDITIONS

Fig. 4 (a, b) shows the experimental assembly used to reproduce the in-service conditions of the SKL-1 fastening system. It is made up of a prestressed concrete sleeper, a segment of a rail and the SKL-1 fastening system that links both. The tests carried out are based on the specifications [15] [16] and consist of two parts. Firstly, the bolts are tightened, recording their vertical displacement. Then, the test consists in repeating a compressive cyclical sinusoidal load with constant amplitude for $3 \cdot 10^6$ cycles at a frequency of 5 Hz, a minimum load of 5 kN and a maximum load of 70 kN. The angle between the load line and the vertical line was 26º (simulating the conditions of passage of a railway vehicle in a curve). The tests were performed with a bench equipped with a dynamic servo-hydraulic actuator, brand INSTRON series 8505, with a loading capacity of ±100 kN. During the test, the vertical displacements undergone by the rail foot (because of the turning of the rail) on the side corresponding to the outside of the curve (which is where the fatigue loading of the clip is more damaging) were continuously recorded by means of two LVDTs, see Fig. 4(a). In addition, the horizontal displacements of the head of the rail were also measured with another couple of LVDTs, see Fig. 4(b). The vertical displacements have been introduced into the FE model of the system to define the boundary conditions (mean displacement, δ_m, and amplitude displacement, δ_a), as sketched in Fig.4(c). According to the specification [15], the test is considered acceptable if the system exceeds $3 \cdot 10^6$ cycles. In this experimental campaign, 12 fatigue tests of this type have been carried out.

(a)

(b)

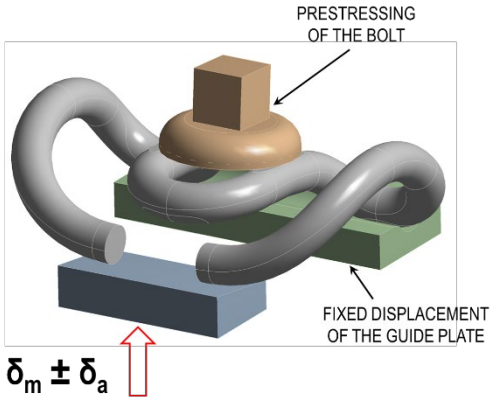

(c)

Figure 4. (a, b) Pictures showing the experimental setup to reproduce the in-service conditions of the fastening system. (c) Schematic description of the boundary conditions imposed in the FE model.

2.4.- STATISTICS

The MATLAB Curve Fitting Toolbox™ software allows the confidence bounds for the fitted coefficients or the prediction bounds for new observations to be calculated. From the S-N curves obtained experimentally (section 3.1.3), the corresponding prediction bounds for different probabilities of failure (1%, 5%, 95% and 99%; respectively) have been calculated to obtain in this way the so-called P-S-N curves [17]. These curves were implemented in ANSYS in order to develop a statistical assessment of the fatigue performance of the SKL-1 clips.

2.5.- FINITE ELEMENTS NUMERICAL SIMULATION

FE numerical simulations were developed in this study by means of the software ANSYS Workbench 18.0. Fig. 5 shows the components included in the model. The mechanical and fatigue properties of the clip correspond to the experimental results obtained through tensile and fatigue tests, including in this case the prediction bounds. The screw and the rail were modelled as Structural Steel (material included in the database provided by ANSYS Workbench). Finally, the mechanical properties of the guide plate, which is fabricated in polyamide 66 reinforced with short glass fiber (35 wt. %), were taken from a previous research by the same authors [18].

The final mesh consists of 190060 nodes and 49097 elements. Each of the components (clip, bolt, rail and guide plate) was meshed independently, but taking into account the mutual interactions (contact regions). The general maximum size of the elements was 3 mm and a hex dominant method was applied to the whole model. Additionally, a Multizone method was used on the bolt, the plate and the rail, aiming at obtaining a regular mesh. A face meshing was added to the plate to ensure the regularity of the elements in the area where the contact with the clip occurs. The mesh was densified in the contact regions between bodies, imposing a maximum element size of 1.5 mm. Three groups of contacts have been defined in the model between the following bodies: clip-bolt, clip-plate and clip-rail. In all cases, the contact was defined as a frictional contact with a coefficient of friction of 0.2. To avoid the interpenetration of the bodies, guaranteeing the contact compatibility, Augmented Lagrange formulation was used.

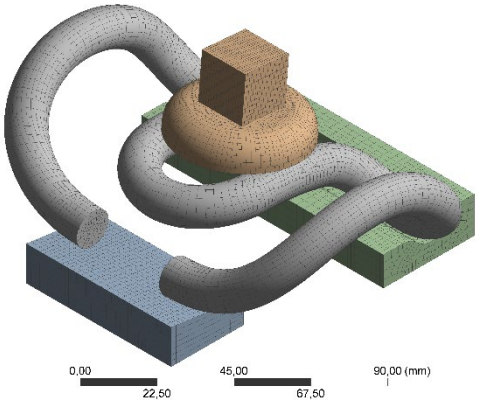

Figure 5. Description of the meshing of the different parts that compose the fastening system.

3.- RESULTS

3.1.- EXPERIMENTAL RESULTS ON STANDARD SPECIMENS

3.1.1.- MICROHARDNESS

Fig. 6 shows a comparison between the Vickers microhardness values obtained along the 6 mm diameter of a cross-section of a tensile specimen and the 13 mm diameter of a SKL-1 clip. As can be seen, the hardness values are virtually indistinguishable. This result underlines the fact that the material of the tensile and fatigue specimens and that of the clip present the same microstructural nature and guarantees the representativeness of the experimental results. In addition, the surface condition of specimens and clips is the same, as they were subjected to the same shot-peening treatment (in the same facilities, indeed).

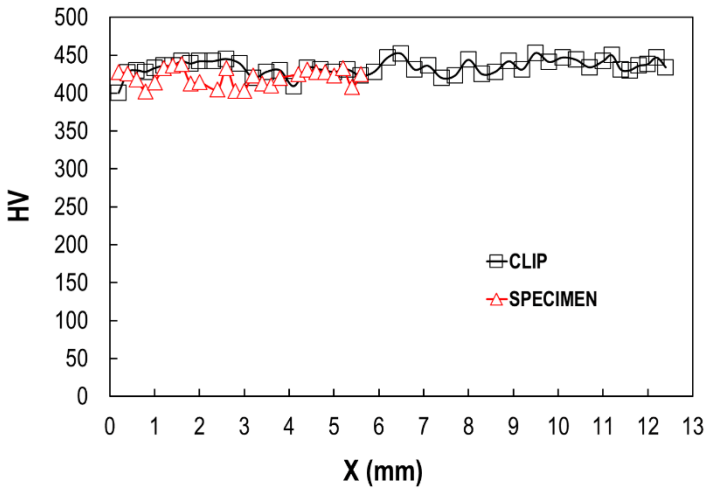

Figure 6. Comparison between the Vickers microhardness profiles obtained in one tensile specimen and in one SKL-1 clip (after subjecting both of them to the same heat and shot-peening treatments).

3.1.2.- TENSILE TESTS

The stress-strain curves are reproduced in Fig. 7. As indicated previously, one of the specimens was tested without receiving any treatment (which is referred to as “non-treated”) while the second had received the quenching and tempering heat treatment as well as the shot-peening (“treated” specimen in the figure). The relevant mechanical parameters are summarized in Table 3. The differences between the two curves are noteworthy: thanks to the applied treatments, a substantial increase in the resistant ability of the material occurs (expressed in terms of yield stress or tensile strength, which increase by 148% and 71%, respectively). The high value of the yield stress is an indispensable requirement for a spring clip since an efficient performance is based on its capacity to resist loads in the linear elastic regime. This improvement in strength takes place at the expense of a reduction in ductility expressed in terms of the strain under maximum load (-63%), although the ultimate strain is virtually not affected (in both cases, ~25%).

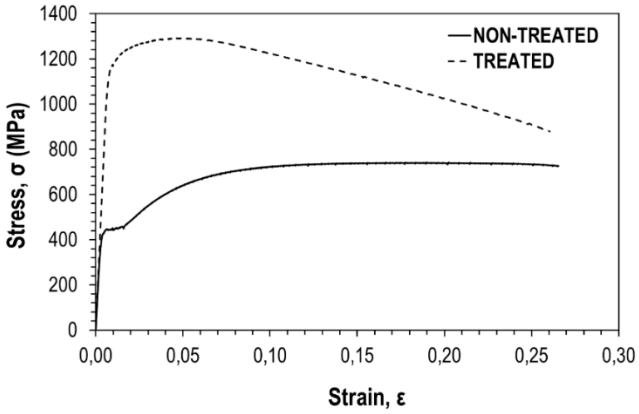

Figure 7: Stress-strain curves obtained from a non-treated and a heat and shot-peened treated specimen.

Table 3. Mechanical properties of the non-treated and treated 38Si7 steel.

	Non-treated	Treated	Variation (%)
Yield Stress (MPa)	434	1077	148
Tensile Strength (MPa)	756	1291	71
Strain under maximum stress	0.139	0.052	-63
Ultimate strain	0.265	0.257	-3

3.1.3.- FATIGUE TESTS

Fig. 8(a) and 8(b) show the experimental data obtained after testing the fatigue specimens with, respectively, mean stress σ_m=0 (or R=-1) and $\sigma_m \neq 0$ (R = 0.1 in this case). In each case, a downward sloping and a horizontal region are observed. These regions follow a straight line in logarithmic scale. The equation of the line in the negative slope region is known as the Basquin model. The horizontal line represents the fatigue (or endurance) limit of the material, σ_e; below σ_e the life of the component is assumed to be infinite. The Basquin equations as well as the corresponding coefficients of determination, R^2, are included in the figures. The comparison between Fig. 8(a) and 8(c) allows the influence derived from the mean stress to be understood; thus, the number of cycles to failure decreases as the stress ratio, R, increases (or, equivalently, as the mean stress, σ_m, increases). This phenomenon is seen in the downward sloping region as well as in the fatigue limit, σ_e, of the material. For R = -1, σ_e = 301 MPa and for R = 0.1 it reduces to σ_e = 291 MPa. The intersection between the Basquin and the endurance regions occurs for N_f ~ 490000 cycles; this means that, disregarding the intrinsic uncertainties of fatigue, once a component subjected to R=-1 uniaxial stresses exceeds this number of cycles, its life is infinite. Fig. 8(c) and 8(d) show the prediction bounds (for the failure probabilities 1%, 5%, 95% and 99%, respectively) of the experimental data.

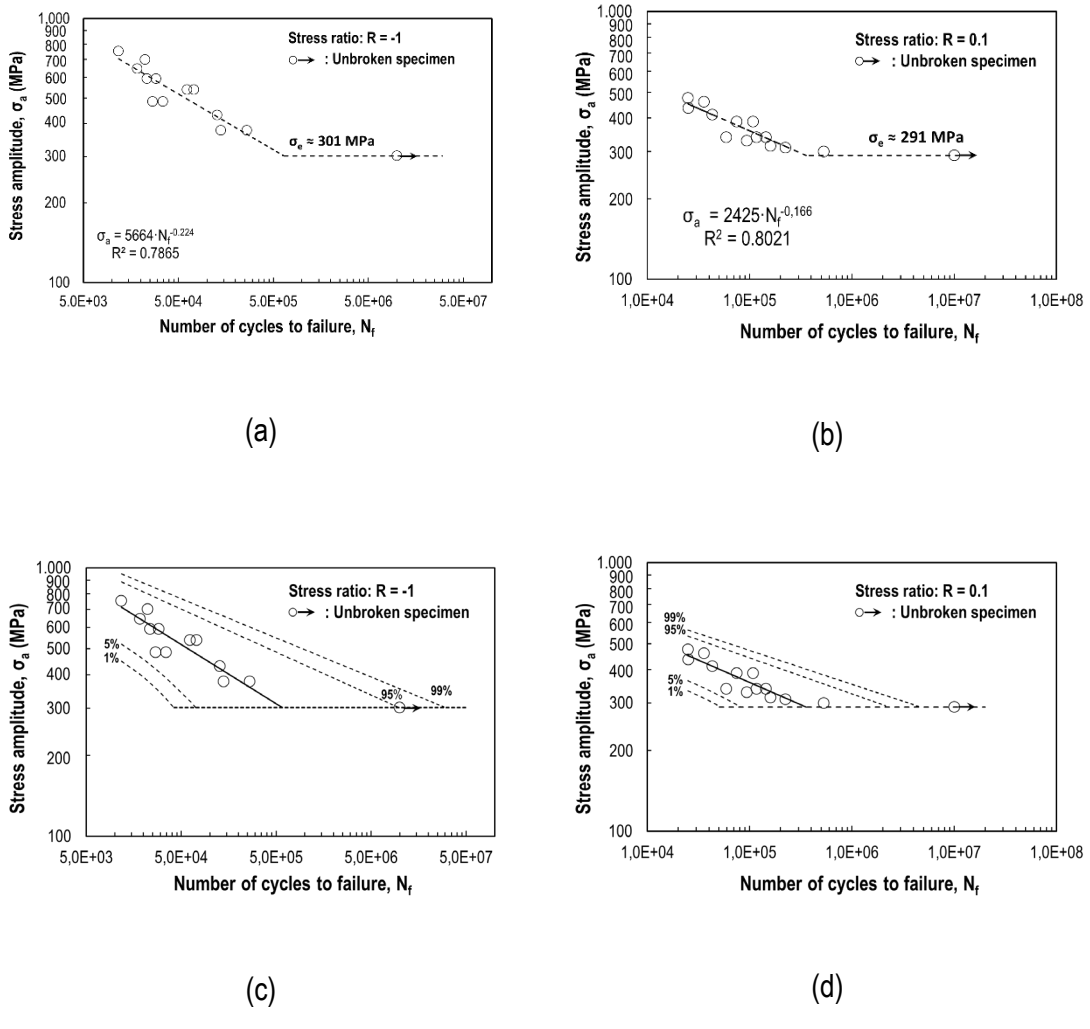

Figure 8. Experimental results obtained from the fatigue characterization, (a) R=-1, (b) R=0.1, and the corresponding prediction bounds, (c) and (d), respectively.

The specialized scientific literature collects various empirical models for metallic materials to correct the effect of the mean stress on fatigue. The three most used models (which are also implemented in the fatigue module of ANSYS Workbench) are those of Soderberg, Goodman and Gerber [19] [20]. These models provide a relationship between the stress amplitude with σ_m=0 ($\sigma_{a(\sigma m=0)}$) and the stress amplitude with $\sigma_m \neq 0$ ($\sigma_{a(\sigma m\neq 0)}$) that produces the same number of cycles until failure. The expressions of the three models, (equations (1) to (3)), are reproduced next

Soderberg: $\sigma_{a(\sigma_m \neq 0)} = \sigma_{a(\sigma_m=0)} \left(1 - \frac{\sigma_m}{\sigma_Y}\right)$ (1)

Goodman: $\sigma_{a(\sigma_m \neq 0)} = \sigma_{a(\sigma_m=0)} \left(1 - \frac{\sigma_m}{\sigma_{TS}}\right)$ (2)

Gerber: $\sigma_{a(\sigma_m \neq 0)} = \sigma_{a(\sigma_m = 0)} \left[1 - \left(\frac{\sigma_m}{\sigma_{TS}}\right)^2\right]$ (3)

where σ_Y is the material's yield stress and σ_{TS} the tensile strength.

There is no universal criterion to decide what correction must be used for a certain metallic material. It is assumed that the Soderberg criterion is overly conservative, that Goodman works well for brittle metals while Gerber is suitable for ductile metals. In this paper, a novel procedure is proposed to select the most suitable corrective method for the steel of the SKL-1 clip based on the experimental results obtained from the fatigue tests.

First, the stress amplitudes for $\sigma_m \neq 0$ have been corrected using the Soderberg, Goodman and Gerber expressions, respectively. Then, using the Basquin fitting for $\sigma_m = 0$, the predictions of the number of cycles until failure were obtained. Both the experimental results (with R = -1 and R = 0.1) and the corrected values are shown in Fig. 9 (a). As can be seen, the experimental data with R=-1 fall between the Goodman's and Gerber's predictions. The novel solution proposed in this study consists in carrying out a linear combination of the Goodman and Gerber methods, with the form "α·Goodman + β·Gerber", where β = 1- α. Then, the value of α has been obtained through a least squares procedure, obtaining α = 0.506 (and, consequently, β = 0.494). Fig.9 (b) shows the result obtained after applying this correction on the data with R=0.1: as can be observed, this procedure provides results that are virtually indistinguishable from the experimental values obtained with R = -1.

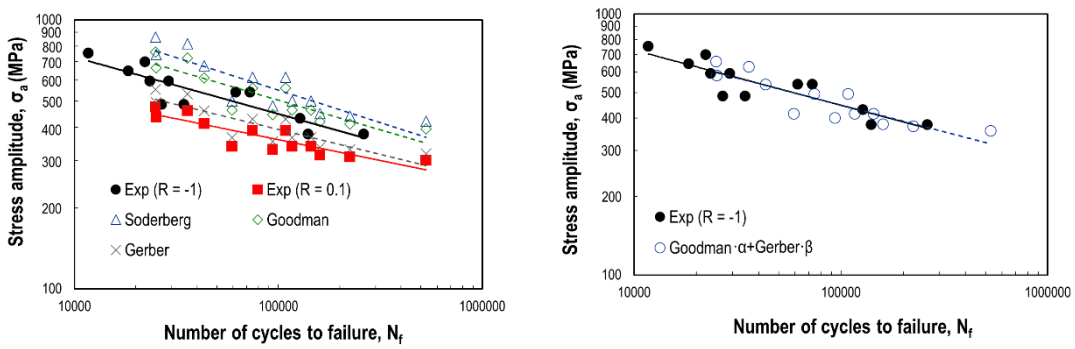

(a) (b)

Figure 9. (a) Experimental data obtained from the fatigue tests (with R=-1 and R=0.1) as well as

the corrected data after applying the Soderberg, Goodman, and Gerber corrections. (b) Comparison between R=-1 data and R=0.1 corrected using a linear combination of Goodman's and Gerber's models.

3.2.- EXPERIMENTAL RESULTS ON CLIPS

3.2.1.- QUASI-STATIC TEST

The experimental curve relating force and displacement is displayed in Fig. 10(a). Initially, the clip responds elastically until a force of ~8 kN; then, the plastic behavior begins. For a displacement of ~15 mm, the contact between the rail and the central region of the clip occurs; for this reason, the slope of the curve notably increases. It is worth noting that this feature is not accidental but a consequence of the design of the clip, which is aimed at preventing the overturning of the rail. After unloading, some plastic deformations remain, given that the elastic limit had been exceeded during loading. The comparison between the experimental results and the predictions obtained from the FE model is displayed in Fig. 10(b). As can be seen, the curve obtained numerically reproduces with precision the experimental curve. In this way, it is concluded that the mechanical validation of the numerical model has been achieved satisfactorily.

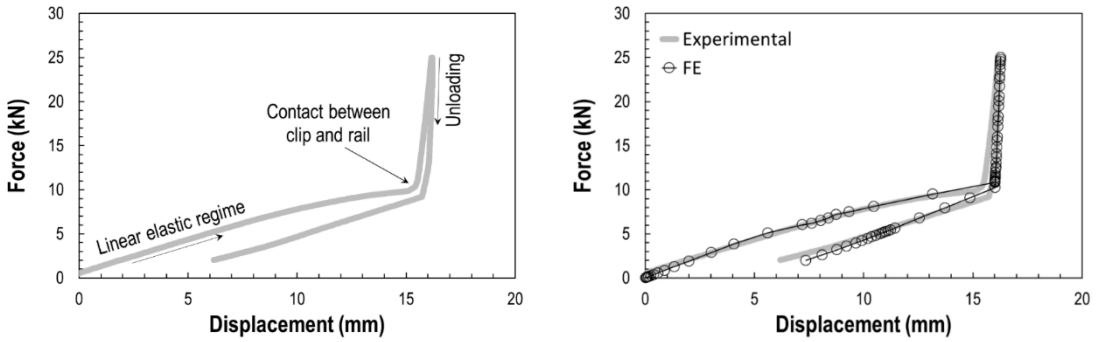

(a) (b)

Figure 10. (a) Experimental curve obtained from the compression test of an SKL-1 spring clip. (b) Comparison between experimental and FE results.

Fig. 11 shows the von Mises stress field for a compression load of 25 kN. This figure allows the

regions where the concentration of stresses occurs to be identified, which correspond to the loops of the SKL-1 spring clip. As can be seen, the maximum stress is 1177 MPa, which exceeds the yield stress of the material (1077 MPa, see Table 3). This result is consistent with the existence of residual deformations detected in the compression test (see Fig. 10) after unloading.

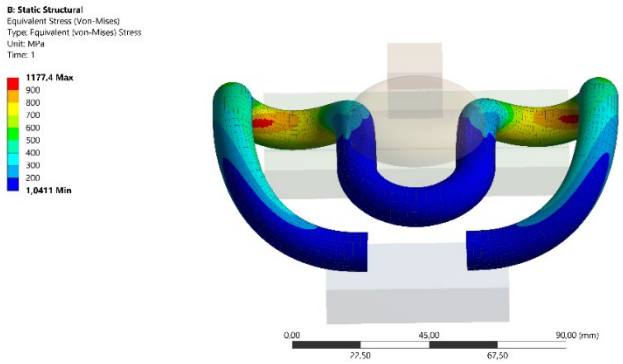

Figure 11. Perspective of the distribution of von Mises stresses for a compression force of 25 kN.

3.2.2.- FATIGUE TESTS

The experimental results derived from the fatigue tests on spring clips are collected in Fig. 12(a). Note that the points (N_f, F_a) follow the same pattern as the S-N curves obtained on standard specimens which consists of a downward sloping and a horizontal region. The coordinate of the horizontal line corresponds to the fatigue limit which is F_e=1200 N (as explained above, this value depends on the mean load during fatigue, F_m=2500 N, in this case). One of the goals of this study is to develop and validate a numerical tool that allows the response to fatigue of the SKL-1 clips under in-service conditions to be assessed. Fig.12(b) shows a comparison between the experimental data and the predictions obtained from the FE model. The fatigue module of ANSYS Workbench receives as input the S-N curves of the material. In order to carry out a statistical evaluation, the fatigue curves associated with different probabilities of failure have been introduced in the model. Besides, the procedure for correcting the effect of the mean stress described in section 3.1.3 has been applied. Finally, to take into account the stress triaxial state in the clip, the von Mises stress has been used. The level of agreement obtained is highly

satisfactory: the experimental data are scattered around the line corresponding with a failure probability of 50% and within the prediction bands. In addition, the model predicts well the fatigue limit of the clip. In conclusion, the FE model has been validated as a tool to evaluate the fatigue behavior of the SKL-1 clip.

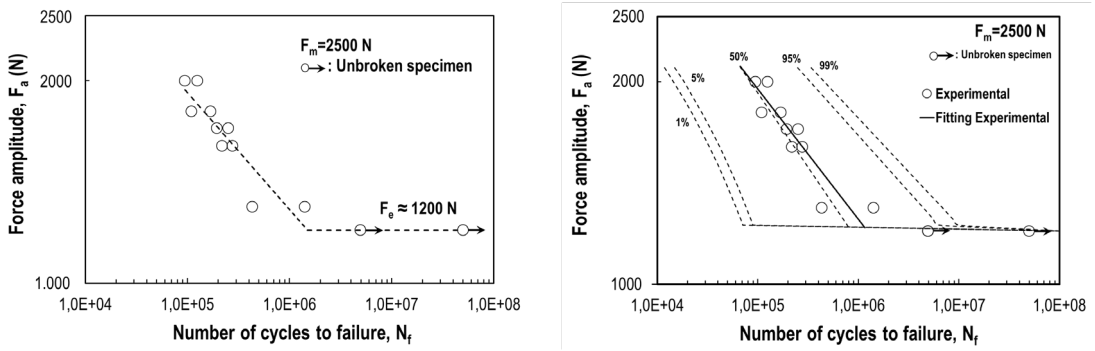

Figure 12. (a) Results of the fatigue tests carried out on SKL-1 spring clips. (b) Comparison between the fatigue results obtained on the spring clip and the predictions provided by the FE model.

2.3.3.- REPRODUCTION OF IN-SERVICE CONDITIONS

As noted above, the result of this fatigue test is considered satisfactory if the component resists $3 \cdot 10^6$ cycles. In this study, 12 fatigue tests have been carried out and, in all cases, the system has verified this condition. After completing the tests, each of the clips has been carefully inspected seeking any evidence that might indicate the existence of an incipient process of fatigue. No evidence of this type been observed. The FE model developed applying the boundary conditions described in section 2.3.2 (Fig.4(c)) allowed the maximum equivalent (thus to say, R=-1) stress amplitude, $\sigma_{a(\sigma m=0)}$ in the clip to be determined, obtaining $\sigma_{a(\sigma m=0)} \approx 134$ MPa. This result is well below the fatigue limit for R = -1, $\sigma_e = 301$ MPa and in fair agreement with the experimental results: as indicated previously, none of the assemblies subjected to fatigue tests reproducing the in-service conditions, underwent any failure nor showed any indication of fatigue

damage.

4.- DISCUSSION AND CONCLUSIONS

The technical literature reports cases of in-service fractures of spring clips of the SKL-1 railway fastening system [1]. This is an element of high responsibility since its failure might imply the derailment of a train, with potentially fatal consequences for passengers and, in any case, a substantial economic loss. This study, which arises from these premises, is aimed at evaluating the conditions of structural integrity of the SKL-1 spring clips under in-service conditions. To this end, an exhaustive research has been carried out including the following sections:

- Characterization of the mechanical and fatigue properties of the steel of the SKL-1 spring clips. To ensure the representativeness of the results, the specimens were subjected to the same thermal and shot-peening treatments as the actual spring clips (in fact, these treatments were applied in the same industrial facility). The fatigue performance of the material was analyzed following a probabilistic description of the S-N curves (referred to as P-S-N approach).
- Characterization of the mechanical (compression test) and fatigue response until failure of a series of spring clips.
- Development and optimization of a FE model, using ANSYS Workbench, to reproduce the structural behavior of the SKL-1 fastening system (including the clip, the foot of the rail, the guide plate and the bolt). This numerical model has been exhaustively validated, both from the mechanical and fatigue viewpoints, using the experimental results described in the previous paragraph.

One of the novel contributions of this study lies in the method applied to model the fatigue behavior. It is a well-known fact that the fatigue life of a structural element depends not only on the stress amplitude but also on the mean stress. The results of this study prove that the fatigue

behavior of the constitutive steel of the SKL-1 spring clips is accurately described using a linear combination of the Goodman's and Gerber's corrective methods.

Both the experimental results and the FE model predictions show that fatigue failure of a spring clip is a highly unlikely event. This result clashes head on with the evidence presented by Lakusic et al. [1]. Experimentally, it has been verified that none of the tests carried out reproducing the in-service conditions has led to the failure of the component, despite having subjected each clip to $3 \cdot 10^6$ cycles. In fact, the beginning of the endurance region of the fatigue curve can be approximately established in $N_f \approx 490000$ cycles; therefore, the experimental conditions imposed by the specifications [15] [16] guarantee that the theoretical lifespan of the component should be infinite. The numerical results agree perfectly with this outcome. Thus, the FE model shows that the maximum corrected stress amplitude in the clip amounts to $\sigma_a \approx 134$ MPa while the endurance limit of the material is $\sigma_e = 301$ MPa.

Given this situation, it is only possible to speculate on the causes behind the failure of spring clips reported by Lakusic et al. [1]. In principle, several possibilities can be pointed out. The most important variable regarding the fatigue resistance is, without a doubt, the material itself. As shown in this paper, in order to achieve adequate mechanical and fatigue properties, it is necessary to apply rigorously a thermal and shot-peening treatments. Both processes must be optimized to avoid compromising the structural integrity of the component. For example, if the yield stress does not reach the required value, the component will work in the plastic regime, which will inevitably reduce its fatigue lifespan as well as its fitness for service. Moreover, a suitable shot-peening treatment is crucial to optimize the fatigue performance. In this sense, two extreme scenarios can be contemplated. In the case of underpeening, the residual compressive stresses are insufficient to prevent the initiation of the cracking process. In contrast, under overpeening conditions, the material may have surface cracks that would accelerate the initiation stage of cracking reducing its lifespan.

The conclusions of our study assume that the assembly of the fastening system has been carried out in accordance with the specifications of the standards [15][16]. These documents detail the characteristics to be satisfied during the prestressing of the clip as well as the testing loads, which are considered representative of the operating conditions. However, nothing avoids the existence of in-service overloads that would reduce the fatigue life of the spring clips. Regardless of the above, the only procedure to elucidate the causes of failures reported by Lakusic et al. [1] would be to carry out a rigorous forensic analysis, based on realistic information about the material properties and in-service loads, including a fractographic evaluation using SEM microscopy.
We do not wish to end this paper without highlighting the fact that the FE numerical model developed and verified in this research would be extensible to any other spring clip geometry, allowing the design stage to be optimized by decreasing deadlines and the costs associated with laboratory tests.

5.- ACKNOWLEDGMENTS

This paper describes the work performed by the Laboratory of Science and Engineering of Materials (LADICIM) of the University of Cantabria (Spain). The authors would like to express their gratitude to the companies Global Steel Wire (GSW), who contributed the rod wire to machine the specimens, and REDALSA, which was responsible for carrying out the heat and shot-peening treatments on the specimens as well as supplying the SKL-1 clips for their characterization.

6.- BIBLIOGRAPHY

[1] Lakusic S, Bartos D, Bajic AG. Experimental an numerical analysis of the rail fastening spring clips types SKL-1 and SKL-12. 22nd Danubia-Adria Symp. Exp. Methods Solid Mech., 2005.

[2] Kang C, Schneider S, Wenner M, Marx S. Development of design and construction of high-speed railway bridges in Germany. Eng Struct 2018;163:184–96. doi:10.1016/j.engstruct.2018.02.059.

[3] Paixão A, Varandas JN, Fortunato E, Calçada R. Numerical simulations to improve the use of under sleeper pads at transition zones to railway bridges. Eng Struct 2018;164:169–82. doi:10.1016/j.engstruct.2018.03.005.

[4] Imam BM, Righiniotis TD, Chryssanthopoulos MK. Numerical modelling of riveted railway bridge connections for fatigue evaluation. Eng Struct 2007;29:3071–81. doi:10.1016/j.engstruct.2007.02.011.

[5] Cheng B, Cao X, Ye X, Cao Y. Fatigue tests of welded connections between longitudinal stringer and deck plate in railway bridge orthotropic steel decks. Eng Struct 2017;153:32–42. doi:10.1016/j.engstruct.2017.10.016.

[6] Hong X, Xiao G, Haoyu W, Xing L, Sixing W. Fatigue damage analysis and life prediction of e-clip in railway fasteners based on ABAQUS and FE-SAFE. Adv Mech Eng 2018;10:1–12. doi:10.1177/1687814018767249.

[7] Chinese National Standard - GB/T1222-2007:2007. Spring steels., n.d.

[8] Yuan F, Liang B, Le J. Elastic-plastic mechanics. Devon: The Yellow River Water Conservancy Press.; n.d.

[9] ET 03.360.566.8, ADIF; 2017.

[10] REDALSA. Especificaciones clip elástico SKL-1 n.d. http://redalsa.com/productos/clip-elastico-skl-1/.

[11] ASTM E92 - 17. Standard Test Methods for Vickers Hardness and Knoop Hardness of Metallic Materials, West Conshohocken, PA: ASTM International; 2017. doi:10.1520/E0092-17.

[12] ASTM E8 / E8M - 16, Standard Test Methods for Tension Testing of Metallic Materials.

ASTM B. Stand., West Conshohocken, PA, 2017: ASTM International; 2016, p. 1–27. doi:10.1520/E0008_E0008M-16A.

[13] ASTM E466 - 15, Standard Practice for Conducting Force Controlled Constant Amplitude Axial Fatigue Tests of Metallic Materials. B. Stand. Vol. 03.01, West Conshohocken, PA: ASTM International; 2015. doi:10.1520/E0466-15.

[14] Lieferbedingungen T. DBS 918 127 2010.

[15] EN 13481-2:2012+A1:2017. Railway applications. Track. Performance requirements for fastening systems - Part 2: Fastening systems for concrete sleepers. CEN, EUROP, 2017, p. 22.

[16] EN 13146-4:2012+A1:2014. Railway applications. Track. Test methods for fastening systems. Effect of repeated loading, 2014, p. 20.

[17] Huang BT, Li QH, Xu SL, Zhou BM. Tensile fatigue behavior of fiber-reinforced cementitious material with high ductility: Experimental study and novel P-S-N model. Constr Build Mater 2018;178:349–59. doi:10.1016/j.conbuildmat.2018.05.166.

[18] Ferreño D, Carrascal I, Ruiz E, Casado JA. Characterisation by means of a finite element model of the influence of moisture content on the mechanical and fracture properties of the polyamide 6 reinforced with short glass fibre. Polym Test 2011;30:420–8. doi:10.1016/j.polymertesting.2011.03.001.

[19] Susmel L, Tovo R, Lazzarin P. The mean stress effect on the high-cycle fatigue strength from a multiaxial fatigue point of view. Int J Fatigue 2005;27:928–43. doi:10.1016/J.IJFATIGUE.2004.11.012.

[20] ASM Handbook, Volume 19: Fatigue and Fracture. Novelty, Ohio: ASM International; 1996.